Analysis of d–d Transitions in *trans*-$[Cr(CN)_2(NH_3)_4](ClO_4)$ as Inferred from Polarized Optical Spectra and Angular Overlap Model Calculations

Thomas Schönherr, Mutsuyoshi Itoh,† and Akio Urushiyama*,†

Institut für Theoretische Chemie, Heinrich-Heine-Universität Düsseldorf, Universitätsstr. 1, D-40225 Düsseldorf, Germany

†Department of Chemistry, College of Science, Rikkyo (St. Paul's) University, Nishiikebukuro 3, Toshima-ku, Tokyo 171

(Received December 21, 1994)

The polarized absorption spectra of *trans*-$[Cr(CN)_2(NH_3)_4](ClO_4)$, which crystallizes in the orthorhombic space group $Pna2_1$, were measured in spin-allowed quartet ($t_{2g}^3 \rightarrow t_{2g}^2 e_g$) and intraconfigurational spin-forbidden doublet ($t_{2g}^3 \rightarrow t_{2g}^3$) transition regions. Gaussian deconvolution of the quartet bands and detailed vibronic assignments of the spin-forbidden doublet transitions yielded a total of seven electronically excited states. These have been used for ligand field calculations in terms of the angular overlap model. By using a π-orbital reduction factor of $\tau=0.984$ as well as a negative e_π value for the acceptor ligand CN^- (-930 cm^{-1}) we were able to reproduce the d-level scheme in high accuracy. The results compare well with our findings for the related monocyano complex.

The ligand field states of acidopentaammine complexes of chromium(III) have been thoroughly studied due to their interesting photochemical behavior. The exceptionally large splitting of the lowest excited state, ^2E_g (O_h), observed in many tetragonal Cr(III) complexes, has been discussed often.[1] The nature of the cyanide ligand concerning its bonding interactions with the central metal ion is also not clear, though π-acceptor behavior has been assumed.[2] Recently, we have reported that the analysis of low-symmetry band splittings in terms of the angular overlap model (AOM) can provide such information.[3] This has been demonstrated in particular for pentaammine complexes of chromium(III) with cyanide and isocyanate hetero ligands.[4,5] Accordingly, in the present contribution, we extended this work to *trans*-$[Cr(CN)_2(NH_3)_4](ClO_4)$ presenting structural data, detailed polarized absorption spectra and a complete AOM analysis of d–d transitions.

Experimental

Preparation of the Compounds. The yellow solid of *trans*-$[Cr(CN)_2(NH_3)_4](ClO_4)$ was prepared according to the literature.[6] The deuterated derivative was obtained by recrystallizing twice from a D_2O solution. Single-crystals suitable for low-temperature polarized absorption measurements and X-ray crystal structure determination were obtained by slow (dispersion) mixing of aqueous solutions of *trans*-$[Cr(CN)_2(NH_3)_4](ClO_4)$ and lithium perchlorate in an U-shaped glass tube, which was stored overnight in a refrigirator (5 °C). Longer growth time cause decomposition of the complex cation.

X-Ray Analysis. The crystal structure analysis of *trans*-$[Cr(CN)_2(NH_3)_4](ClO_4)$ was performed by using a Rigaku AFC-5 four-circle automated diffractometer. A total of 1065 independent reflections was collected by a ω–2θ scan mode ($2° < 2\theta < 55°$) and the absorption correction by North et al. was applied.[7] The locations of all non-hydrogen atoms were determined by an ordinary heavy atom method and refined by a block-diagonal least-square method with anisotropic temperature factors (R value 0.049). All computational work was done by a HITAC 682H computer at the Computer Center of the University of Tokyo using a library program system for X-ray crystallography (UNICS III).[8] The difference Fourier maps did not reveal the positions of the hydrogen atoms clearly even at the final stage, probably as a consequence of rotations around the Cr–NH_3 axes. Results of the X-ray analysis are presented in Tables 1 and 2. Tables of thermal parameters and F_o and F_c are given in the supplementary materials, which are deposited as Document No. 68036 at the Office of the Editor of Bull. Chem. Soc. Jpn.

Spectroscopic Measurements. The polarized absorption spectra of single-crystals of *trans*-$[Cr(CN)_2(NH_3)_4](ClO_4)$ were measured by using the instrumentation and methods described previously.[4] Polarized spin-allowed transitions were obtained from thin crystal plates in different polarizations (A, B), they are depicted in Fig. 1. Sharp-line spectra of the low energy intercombination band region are presented in Fig. 2. Also included is the unpolarized spectrum of the deuterated derivative (D) as well as the very weak absorption bands in the higher energy region between 15600 and 18200 cm^{-1} (H) that illustrates the detailed band

Table 1. Prositional Parameters of *trans*-[Cr(CN)$_2$(NH$_3$)$_4$](ClO$_4$)

Atom	x	y	$-z$	B_{eq}[a)]
Cr	−0.2264(1)	−0.0006(12)	−0.0637(1)	1.3
C1(CN1)	−0.0289(9)	0.0024(66)	0.0135(7)	1.9
C2(CN2)	−0.4232(10)	−0.0016(53)	0.1158(7)	2.2
N1(CN1)	0.0795(9)	0.0034(64)	−0.0098(7)	3.1
N2(CN2)	−0.5288(9)	−0.0007(54)	0.1462(8)	3.7
N1	−0.1751(39)	0.1847(43)	0.1644(29)	1.9
N2	−0.1715(39)	−0.1927(46)	0.1657(29)	2.6
N3	−0.2699(30)	−0.1961(50)	−0.0412(33)	2.2
N4	−0.2813(30)	0.1913(51)	−0.0350(33)	2.1
C1	−0.0571(2)	−0.0001(18)	−0.2789(2)	1.9
O1	−0.0947(31)	−0.1490(33)	−0.2253(28)	2.6
O2	−0.1017(36)	0.1537(36)	−0.2246(32)	3.0
O3	0.0846(8)	−0.0135(42)	−0.2890(7)	2.9
O4	−0.1191(11)	−0.0008(44)	−0.3749(5)	4.6

a) $B_{eq}=(4/3)$ trace(Beta×G)×10^2.

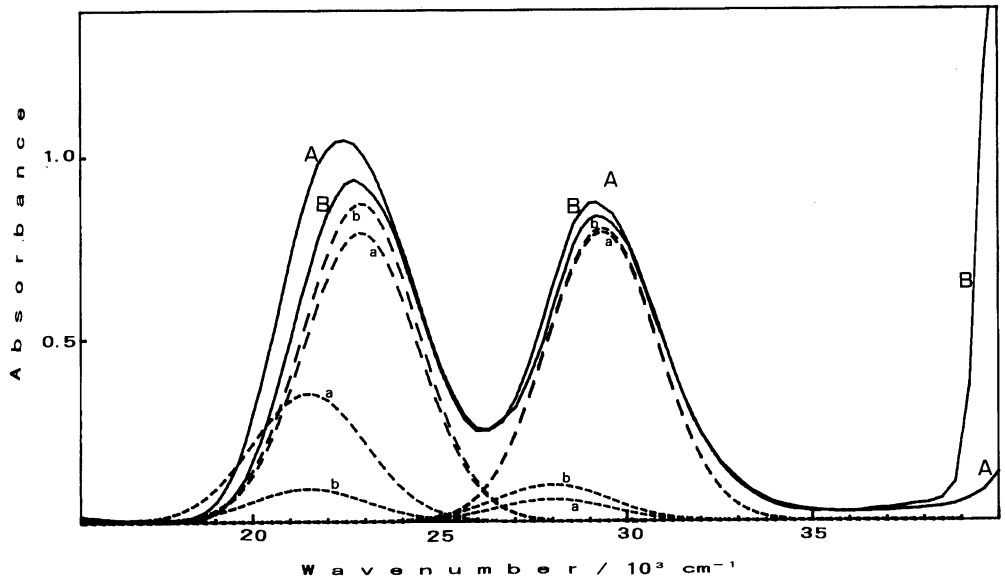

Fig. 1. Polarized absorption spectra of *trans*-[Cr(CN)$_2$(NH$_3$)$_4$](ClO$_4$) in the spin-allowed transition region at room temperature. Sample dimensions are 1.00×0.25×0.004 (optical thickness) mm. A: by the polarized light propagating perpendicular to the crystal (101) face with the electric vector parallel to the [010] axis (b-axis). B: parallel to the crystal [101] axis. Gaussian analyses are given for either spectrum. The analyses were performed with the assumption that all of the band components have the same half-width.

pattern of these spin-forbidden transitions. Measurements of the IR and Raman spectra were performed similar to previous work[4)] including a full normal coordinate analysis of the cation which considers also the hydrogen atoms in the ammine groups. Experimental and calculated vibrational frequencies are collected in Table 3.

Results and Discussion

Molecular Structure. The compound crystallizes in the non-symmorphic orthorhombic space group $Pna2_1$ (C_{2v}^9). The lattice parameters are found to be $a=1008.8$, $b=783.1$, and $c=1354.3$ pm with four formulas per unit cell ($Z=4$). The measured density of $D_m=1.67$ g cm^{-3} fits the calculated value of $D_c=1.68$ g cm^{-3}. All atoms including the central chromium atom are located at general positions, resulting in a C_1 crystallographic symmetry of the complex. However, for d-level calculations the actual structure of the cation can effectively be considered to be close to D_{4h}.

Spin-Allowed Transitions. The tetragonal contribution of the cyanide ligands to the ligand field potential causes an optical anisotropy. This is illustrated in Fig. 1, where slightly different band shapes for A- and B-polarization are shown in the spin-allowed region of $^4A_{2g}\rightarrow{}^4T_{2g}$, $^4T_{1g}$ transitions (in O_h notation) of the single-crystal absorption spectrum. According to the results of the X-ray crystal structure analysis, the A-polarized spectrum of the present measurements (see footnote of Fig. 1) is almost the pure molecular xy-polarized spectrum of the uniaxial chromophore (D_{4h} symmetry).

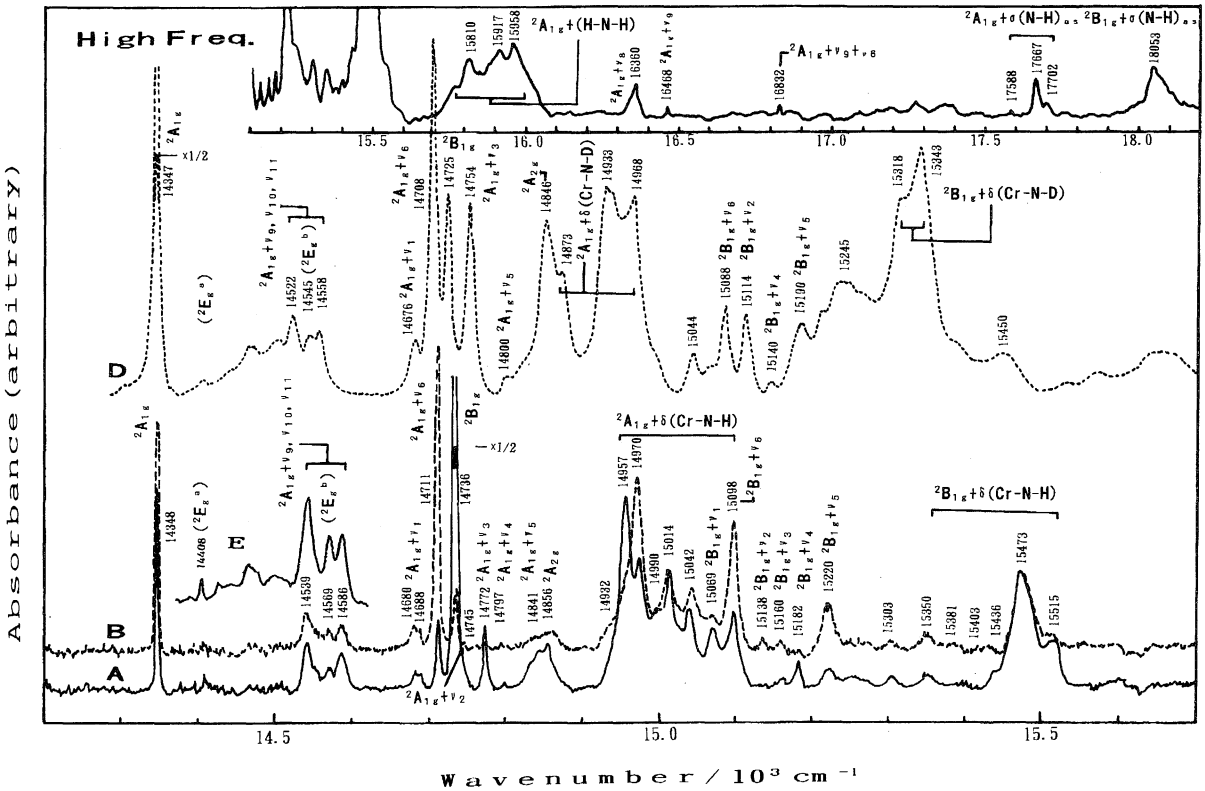

Fig. 2. Crystal absorption spectra of *trans*-$[Cr(CN)_2(NH_3)_4](ClO_4)$ in the region of t_{2g}^3 intraconfigurational transitions measured at 78 K. Sample dimensons (mm): 1.00×0.25×1.20 (=opticalthickness). A and B as described for Fig. 1. D: Unpolarized spectrum of microcrystalline sample of the deuterated derivative. High Freq: Microcrystalline spectrum (H-compound) in the higher wavenumber part of the (vibronic) spin-forbidden transitions. E: Unpolarized spectrum under the same condition as High Freq. Assignments of the five electronic origins and vibronic side-bands are included.

Table 2. Bond Lengths (in pm) and Bond Angles (in °) in *trans*-$[Cr(CN)_2(NH_3)_4](ClO_4)$

Cr–C1	211(1)	C1–Cr–C2	179(1)
Cr–C2	211(1)	Cr–C1–N1	177(1)
Cr–N1	206(4)	Cr–C2–N2	178(2)
Cr–N2	212(4)	C1–Cr–N1	88(1)
Cr–N3	213(4)	C1–Cr–N2	88(1)
Cr–N4	209(4)	C1–Cr–N3	89(1)
C1–N1 (CN1)	116(1)	C1–Cr–N4	92(1)
C2–N2 (CN2)	114(1)	N1–Cr–N2	90(1)
		N2–Cr–N3	89(1)
		N3–Cr–N4	92(2)
		N1–Cr–N4	89(2)

The B-polarized spectrum, however, is a superposition of the *z*-spectrum (68%) and of the *xy*-spectrum (32%). A clear splitting of the quartet bands can not be detected. However, a Gaussian band deconvolution of the absorption pattern yielded maxima for the tetragonal components of $^4T_{2g}$ and $^4T_{1g}$ at 21500, 22900 cm^{-1} and 28000, 29350 cm^{-1}, respectively (cf. Fig. 1). This result is supported by arguments which consider vibronic selection rules for the actual D_{4h} symmetry of the *trans*-$[Cr(CN)_2N_4]^+$chromophore in which the skeletal vibrations transform as $3a_{1g}+b_{1g}+b_{2g}+2e_g+3a_{2u}+b_{2u}+4e_u$. If the electric vector of the propagating light is orientated perpendicular to the molecular tetragonal axis, the spin-allowed transition from $^4B_{1g}(D_{4h})$ ground state to any quartet excited state can gain vibronic intensities by promoting modes of proper symmetry. In the molecular *z*-direction, on the other hand, a vibronic mechanism can not account for the transitions $^4B_{1g}\rightarrow{}^4B_{2g}$, $^4A_{2g}$ (in D_{4h} notation). This behavior is qualitatively reflected by our band deconvolution, which shows only weak features at the lower energy side of both quartet bands in the B-spectrum (68% *z*-spectrum). The polarization of the $^4B_{1g}\rightarrow{}^4A_{2g}$ transition that appears slightly higher in the B-spectrum than in the A-spectrum is probably caused by actual low symmetry of the chromophore in the present crystal lattice (C_1). In fact, this transition is statically (i.e., by a pure electronic mechanism) allowed in the z-direction for D_4 or lower symmetries. Thus, we propose level ordering for the quartet states:

$$^4B_{2g} < {}^4E_g{}^a \ll {}^4A_{2g} < {}^4E_g{}^b.$$

This ordering of the higher quartet levels is opposite to the situation with *trans*-$[CrF_2(en)_2]^+$ [9] as expected from the different positions of axial and equatorial ligands in the spectrochemical series, where $D_q(F^-)<D_q(NH^3)<D_q(CN^-)$ holds.

Table 3. Infrared Absorption and Raman (R) Frequencies (ν/cm^{-1}) of *trans*-[Cr(CN)$_2$(NH$_3$)$_4$](ClO$_4$)

Notation	H	D	H/D	Calcd (H-compd)
$\nu_{11}(b_{2u})$: δ(C–Cr–N)				185
$\nu_{10}(e_u)$: δ(N–Cr–N)	215			217
$\nu_9(a_{2u})$: δ(C–Cr–N)	236	215	1.09	231
$\nu_8(b_{2g})$: δ(N–Cr–N)	260 (R)	234 (R)	1.11	263
$\nu_1(a_{1g})$: σ(Cr–N)	330 (328R)	325 (326R)	1.11	263
$\nu_6(e_u)$: δ(Cr–C–N)	356	356	1.01	339
	363 (ab)	363 (ab)	1.00	
$\nu_7(e_g)$: δ(Cr–C–N)	395	385	1.03	351
$\nu_2(a_{1g})$: σ(Cr–N)	418 (R)	383 (R)	1.09	397
$\nu_3(b_{1g})$: σ(Cr–N)	424 (ab)	407 (ab)	1.04	372
$\nu_4(a_{2u})$: σ(Cr–N)	445	417	1.07	470
$\nu_5(e_u)$: σ(Cr–N)	485	465	1.04	500
ρ(Cr–NH$_3$)	733	588	1.25	746
	1283			
δ(H–N–H)$_{as}$	1303	990	1.32	1104—1356
	1338			
δ(H–N–H)$_s$	1615	1175	1.37	1630
	2020	2003	1.01	2082
σ(C–N)	2138	2132	1.00	2083
	2146	2138	1.00	
σ(N–H)$_s$	3185	2295	1.39	3130
	3265	2360	1.38	
σ(N–H)$_{as}$	3320	2450	1.36	3256—3300
ClO$_4^-$	(465, 625, 928, 1120)			

Spin-Forbidden Transitions. Figure 2 gives an impression of the rich vibronic fine structure which is due to the lowest intraconfigurational transitions. Although details are not described here, the analysis of the intraconfigurational transitions can be performed in a manner very similar to that performed for the related cyanopentaammine complex.[4] The characteristic intense sharp lines at 14348 cm^{-1} (14347: D-compound) and 14736 cm^{-1} (14725: D-compound) are identified with the zero-phonon transitions into the tetragonal split levels $^2A_{1g}$ and $^2B_{1g}$ (or the Kramers doublets Γ_7 and Γ_6, respectively, if spin-orbit coupling is considered) of $^2E_g(O_h)$. In fact, towards higher energy most features in the intercombination region can be interpreted in terms of a vibrational sideband structure (fundamentals and combinations) based upon these two zero-phonon transitions (cf. Fig. 2). But, the line at 14856 cm^{-1} (*D*: 14846) should certainly belong to one of the three split levels of $^2T_{1g}(O_h)$, most probably to $^2A_{2g}(D_{4h})$ (see below), because several higher peaks are related also to that origin as vibrational sidebands. We note that all assigments are strongly supported by the experimental deuterium shifts. The identification of the two remaining origins, Γ_6, Γ_7 of $^2E(^2T_{1g})$, can not be derived in the same manner, because the intense vibronic structure of $^2E_g(O_h)$ covers most of the features arising from the components of $^2T_{1g}(O_h)$. Moreover, the location of the $^2E(^2T_{1g})$ split levels is rather dependent on the difference in the axial and equatorial contributions of the ligand field potential.[9] This point will be treated in the next section.

AOM Calculations. Using guidelines for applying the AOM on d–d spectra as given in Refs. 3 and 4, we have confirmed that the experimental splittings of 1300 cm^{-1} for both quartet bands of *trans*-[Cr(CN)$_2$(NH$_3$)$_4$]$^+$ are reproduced only if a negative value for e_π(CN$^-$) is assumed. This situation was reported recently also for [Cr(CN)(NH$_3$)$_5$]$^{2+}$.[4] It is noted that the splitting of the first spin-allowed band ($^4T_{2g}$) is twice as large in the present complex when compared with the monocyano complex (680 cm^{-1}), in full accord with predictions of the ligand field model.[10]

In order to determine the e_σ- and e_π-parameters for the cyanide ligand more precisely, we have also to consider further electronic levels, which are given here by the spin-orbit components of $^2E_g(O_h)$ and $^2T_{1g}(O_h)$. At this stage, the calculation is not straightforward, since it is known that doublet splittings in tetragonal chromium(III) complexes can be crucially influenced by low-symmetry effects embodied in the interelectronic repulsion terms, which are inadequately described within the conventional ligand field theory. Pursuing an idea of

Atanasov,[10] Schmidtke et al.[1] have shown that unusual large splittings of $^2E_g(O_h)$ can be reproduced only if π–orbital expansion factors are included into the inter-electronic repulsion part of the perturbation matrices. For reasons of symmetry, only one new parameter is required for the present complex: the orbital reduction factor $\tau=\tau_{xz}=\tau_{yz}<1$, which considers the pronounced π delocalization of metal-t_{2g} electrons towards the axial CN^- ligands (there is no effect in the equatorial plane, where π-bonding is reasonably neglected, i. e., $e_\pi(NH_3)=0$). Assuming a plausible value for the spin-orbit coupling constant ($\zeta=200$ cm^{-1}) and using the familiar relation

$$10D_q = 3e_\sigma - 4e_\pi,$$

we obtain a further reduction of the parameter space. Because the ligand field strengths are known from the positions of the first spin-allowed transition in the respective octahedral complexes, and because geometrical parameters are not needed here since the molecular structure was determined for the present complex, only two parameters, i. e., the orbital expansion coefficient τ and AOM parameter $e_\pi(CN^-)$, have to be varied in order to fit the measured d–d transitions for *trans*-[Cr(CN)$_2$(NH$_3$)$_4$]$^+$.

A respective two-dimensional contour diagrams is depicted in Fig. 3. This allows the evaluation of the underlying parameters. In order to identify the excited states by their symmetries, these calculations were performed for D_{4h} symmetry, which is very near to the actual molecular structure. The bold lines in Fig. 3 show the dependency of the splitting of $^2E_g(O_h)$ on these parameters. Obviously, the experimentally obtained value

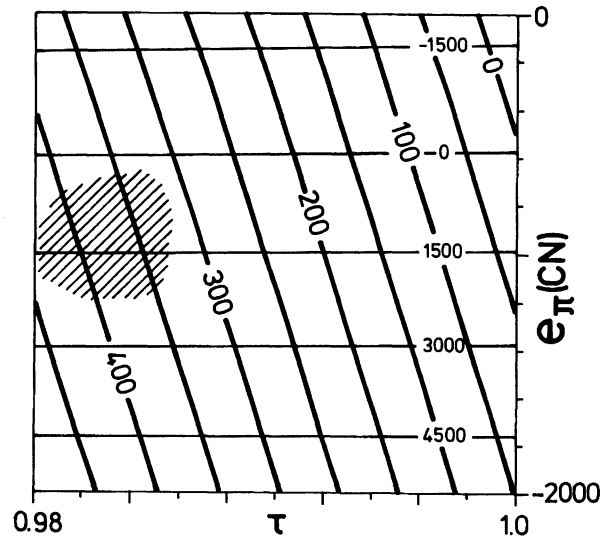

Fig. 3. Contour plot for the ^2E_g (bold line) and for the $^4T_{1g}$ splitting due to the variation of the orbital expansion factor τ and the π interaction with the cyanide ligands (see text). Fixed parameter values: B= 580; C=3500, ζ=200, $D_q(CN^-)$=2630, $e_\sigma(NH_3)$= 7200, $e_\pi(NH_3)$=0; (in cm^{-1}).

of 363 cm^{-1} (361 cm^{-1} for the D-compound) can not be reproduced when the orbital expansion effect is ignored ($\tau=1$). Otherwise, τ values lower than 0.99 may describe the doublet splitting here, in agreement with earlier results on other halogenoammine complexes of chromium(III).[1,4,7] Contour lines for the energy separation of the low-symmetry components of $^4T_{1g}(O_h)$ are included in the plot; these show a strong dependency only on the metal-ligand interaction parameter $e_\pi(CN^-)$. The marked region includes parameter sets which allow for a reasonable description of the experimentally obtained d–d transitions (see below).

Further information should be expected from the positions of the Γ_6, Γ_7 spin-orbit split levels of $^2E_g(^2T_{1g})$. However, the location of these states from the absorption spectra of chromium(III) complexes remains questionable due to the generally very small intensity of the respective zero-phonon and/or vibronic transitions. For example, the emission spectrum of *trans*-[CrF$_2$(en)$_2$](ClO$_4$) clearly originates from a component of $^2E_g(^2T_{1g})$, which, in fact, could not be detected in the respective absorption spectrum.[11] In order to find here a reasonable guess for the location of $^2E_g(^2T_{1g})$ split levels, we have performed a sample calculation by using the parameters for the pentaammine complex, and changing the AOM parameter for the axial trans-ligand from the values for NH_3 to those of CN^-. As result, the components of $^2E_g(^2T_{1g})$, which should be split by more than hundred wavenumbers, are expected to occur between the split levels of $^2E_g(O_h)$, most probably around 14500 cm^{-1} (Table 4). In this part of the absorption spectrum, several weak transitions were detected. These may, however, be assigned as vibrational sidebands (lattice modes) of $^2A_{1g}(\Gamma_7)$. Moreover, there is also no clear evidence of higher vibronic lines based on these (additional zero-phonon) transitions. There-

Table 4. Observed and Calculated d–d Transitions in *trans*-[Cr(CN)$_2$(NH$_3$)$_4$](ClO$_4$)
Optimized Parameters: $e_\pi(CN)=-930$, $B=580$, $C=3565$, $\tau=0.984$. Fixed Values: $D_q(CN)=2630$, $\zeta=200$, $e_\sigma(NH_3)=7200$, $e_\pi(NH_3)=0$ (in cm^{-1})

Energy level	Exptl	Calcd	Dev.
$^2A_{1g}(\Gamma_7)$	14348	14353	5
$^2B_{1g}(\Gamma_6)$	14736	14737	1
$^2E_g(O_h)$ splitting	388	384	−4
$^2E_g^a(\Gamma_7)$	14408[a)]	14433	25
$^2E_g^b(\Gamma_6)$	14569[a)]	14570	1
$^2A_{2g}(\Gamma_6)$	14856	14817	−39
$^2T_{1g}$–^2E_g splitting	508	464	−44
$^4B_1$	21500	21560	60
$^4E^a$	22900	23740	840
$^4T_{2g}(O_h)$ splitting	1400	2180	780
$^4A_2$	28000	28390	390
$^4E^b$	29350	29690	340
$^4T_{1g}(O_h)$ splitting	1350	1350	0

a) Tentative assignment (see text).

fore, we were not able to prove distinct assignments for these states which may be identified, nevertheless, with some weak features in this spectral region.

Finally, by using the fitting routine described in our preceding paper[4] we obtained a good fit# for all experimentally determined quartet and doublet levels of *trans*-$[Cr(CN)_2(NH_3)_4]^+$. The results presented in Table 4 are in line with the previously analysed $[Cr(CN)(NH_3)_5]^{2+}$ and other halogenopentaamine complexes of chromium(III).[1,3,4] The strong covalency connected with the axial ligands is reflected here by a further lowering of the interelectronic parameters B and τ. We note that the parameter values determined in our series of works on cyano-complexes of chromium(III) appear to be rather significant as derived from the basis of a manifold of quartet and doublet transitions which were obtained from highly resolved single-crystal absorption spectra.

We are grateful to Mr. Keiichi Mizutani and Dr. Kazumasa Harada, Rikkyo (St. Paul's) University, for their help on the X-ray crystal structure analysis of *trans*-$[Cr(CN)_2(NH_3)_4](ClO_4)$. Financial support of the Deutsche Forschungsgemeinschaft, Bonn, is gratefully acknowledged.

References

1) H. -H. Schmidtke, H. Adamsky, and T. Schönherr, *Bull. Chem. Soc. Jpn.*, **61**, 59 (1988).
2) L. G. Vanquickenborne and A. Ceulemans, *Coord. Chem. Rev.*, **48**, 159 (1983).
3) T. Schönherr, "Applications of the Angular Overlap Model," in "Topics in Current Chemistry," ed by H. Yersin, Springer, Berlin, in press.
4) A. Urushiyama, M. Itoh, and T. Schönherr, *Bull. Chem. Soc. Jpn.*, **68**, 594 (1995).
5) T. Schönherr, R. Wiskemann, and D. Mootz, *Inorg. Chim. Acta*, **221**, 85 (1994).
6) P. Riccierei and E. Zinato, *Inorg. Chem.*, **19**, 853 (1980).
7) A. T. C. North, D. C. Philips, and F. S. Mathews, *Acta Crystallogr. Sect. A*, **A24**, 351 (1968).
8) T. Sakurai and K. Kobayashi, *Rep. Inst. Phys. Chem. Res. (Jpn.)*, **55**, 69 (1970).
9) L. Dubicki and P. Day, *Inorg. Chem.*, **10**, 2023 (1971).
10) M. A. Atanasov, unpublished results.
11) C. D. Flint and A. P. Matthews, *J. Chem. Soc., Faraday Trans. 2*, **70**, 1307 (1974).

#The fit could be further improved by using a reduced value for $10D_q(CN)$, however, the relatively small splitting of the first quartet band was not obtained from measured band maxima by means of a band deconvolution.